THE JOURNAL OF BIOLOGICAL CHEMISTRY
Vol. 280, No. 5, Issue of February 4, pp. 3138–3142, 2005

Printed in U.S.A.

HDQ (1-Hydroxy-2-dodecyl-4(1*H*)quinolone), a High Affinity Inhibitor for Mitochondrial Alternative NADH Dehydrogenase

EVIDENCE FOR A PING-PONG MECHANISM*[S]

Received for publication, September 30, 2004, and in revised form, November 4, 2004
Published, JBC Papers in Press, November 8, 2004, DOI 10.1074/jbc.M411217200

Andrea Eschemann‡, Alexander Galkin‡, Walter Oettmeier§, Ulrich Brandt‡, and Stefan Kerscher‡¶

From the ‡Universität Frankfurt, Fachbereich Medizin, Institut für Biochemie I, Frankfurt am Main D-60490, Germany and §Ruhr-Universität Bochum, Lehrstuhl für Biochemie der Pflanzen, Bochum D-44780, Germany

Alternative NADH dehydrogenases (NADH:ubiquinone oxidoreductases) are single subunit respiratory chain enzymes found in plant and fungal mitochondria and in many bacteria. It is unclear how these peripheral membrane proteins interact with their hydrophobic substrate ubiquinone. Known inhibitors of alternative NADH dehydrogenases bind with rather low affinities. We have identified 1-hydroxy-2-dodecyl-4(1*H*)quinolone as a high affinity inhibitor of alternative NADH dehydrogenase from *Yarrowia lipolytica*. Using this compound, we have analyzed the bisubstrate and inhibition kinetics for NADH and decylubiquinone. We found that the kinetics of alternative NADH dehydrogenase follow a ping-pong mechanism. This suggests that NADH and the ubiquinone headgroup interact with the same binding pocket in an alternating fashion.

Alternative NADH dehydrogenases (NADH:ubiquinone oxidoreductases) are respiratory chain enzymes that carry out the same redox reaction as mitochondrial complex I. However, unlike this complicated multi-subunit enzyme, they do not contribute to the proton gradient across the respiratory membrane and are insensitive to complex I inhibitors like rotenone and piericidin A (for an overview see Ref. 1). Alternative NADH dehydrogenases are inhibited by flavones in the micromolar range. Acridones have been demonstrated to inhibit both complex I and alternative enzymes (2).

Alternative NADH dehydrogenases are found in the respiratory chains of plants (3), fungi (4–7), many eubacteria (8, 9), and archaebacteria (10–12). They consist of a single polypeptide chain that exhibits no obvious transmembrane domains and contains one molecule of FAD with the exception of the archaebacterial enzymes that, presumably as an adaptation to thermic habitats, carry covalently attached FMN instead.

In most plants and fungi, multiple isoforms of NADH dehydrogenases are expressed in the same species. The active site of the membrane-associated enzymes may be directed to the external or internal face of the mitochondrial inner membrane. In *Saccharomyces cerevisiae*, for example, two external (SCNDE1 and SCNDE2) and one internal (SCNDI1) alternative NADH dehydrogenases are found (13). The obligate aerobic yeast *Yarrowia lipolytica* has only a single external alternative enzyme, YLNDH2 (5). It has been demonstrated that this external enzyme can be transformed into an internal version simply by adding a targeting signal for the mitochondrial matrix (14). This suggests that there are no specific protein interaction partners for its membrane association. It remains unclear how the largely hydrophilic enzyme interacts with its highly hydrophobic substrate, ubiquinone. NADH, the other substrate of alternative NADH dehydrogenases, is highly hydrophilic.

Inspection of the YLNDH2 sequence revealed two $\beta\alpha\beta$-dinucleotide-binding domains that consist of two parallel β-strands connected by an α-helix (5). The sequence G(*X*)*X*G*XX*G, which marks the connection between the first β-strand and the connecting α-helix, makes close contact with the diphosphate moiety of dinucleotide substrates or cofactors. The end of the second β-strand is often occupied by an acidic residue, which forms hydrogen bonds to the 2′- and 3′-hydroxyl groups of the adenine ribose (15). In the amino-terminal dinucleotide fold of *Y. lipolytica* NDH2, the acidic residue is replaced by serine. It has been suggested that this motif binds FAD (8). This proposal is consistent with the position of the FAD cofactor in the crystal structure of two different homologous lipoamide dehydrogenases (16, 17).

In the *Escherichia coli* sequence, a patch of highly basic amino acids that may contribute to membrane attachment by electrostatic interactions is found downstream of the G(*X*)*X*G*XX*G motif at positions 30–35. This pattern is missing at the corresponding position in *Y. lipolytica* NDH2, but the clustering of basic amino acids is observed immediately upstream of this motif. Two conserved regions almost exclusively consisting of apolar and aromatic residues have been proposed to form a possible interaction site for the hydrophobic substrate ubiquinone (5). However, no evidence is available that would experimentally identify the domains forming a binding pocket for the hydrophobic substrate ubiquinone.

Here we have characterized HDQ[1] (1-hydroxy-2-dodecyl-4(1*H*)quinolone) as a novel high affinity inhibitor of membrane-bound NDH2 from *Y. lipolytica* and analyzed the mechanism of alternative NADH:ubiquinone oxidoreductases by bisubstrate and inhibition steady-state kinetics.

* This work was supported by the Deutsche Forschungsgemeinschaft, Sonderforschungsbereich 472. The costs of publication of this article were defrayed in part by the payment of page charges. This article must therefore be hereby marked "*advertisement*" in accordance with 18 U.S.C. Section 1734 solely to indicate this fact.

[S] The on-line version of this article (available at http://www.jbc.org) contains supplemental equations and tables.

¶ To whom correspondence should be addressed: Universität Frankfurt, Fachbereich Medizin, Institut für Biochemie I, Theodor-Stern-Kai 7, Haus 25B, D-60590 Frankfurt am Main, Germany. Tel.: 49-69-6301-6943; Fax: 49-69-6301-6970; E-mail: kerscher@zbc.kgu.de.

[1] The abbreviations used are: HDQ, 1-hydroxy-2-dodecyl-4(1*H*)quinolone; DBQ, *n*-decylubiquinone; DQA, 2-decyl-4-quinazolinyl amine; Mops, 4-morpholinepropanesulfonic acid.

TABLE I
Catalytic activities of NDH2 with different electron acceptors

Acceptor	Activity		+ 10 μM HDQ
	μmol min⁻¹ mg⁻¹	*%*	*% Inhibition*
DBQ	1.4 ± 0.3	100	82 ± 3
Ubiquinone-1	2.1 ± 0.4	152 ± 4	79 ± 2
Duroquinone	0.7 ± 0.2	53 ± 8	23 ± 13
Menadione	0.7 ± 0.2	53 ± 5	No inhibition
Dichlorophenol-indophenol	1.5 ± 0.3	111 ± 5	15 ± 3

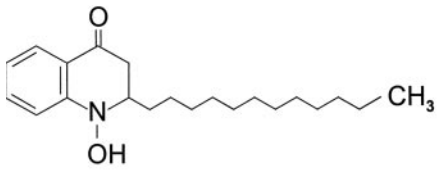

1-hydroxy-2-dodecyl-4(1H)quinolone

FIG. 1. **Structure of HDQ.**

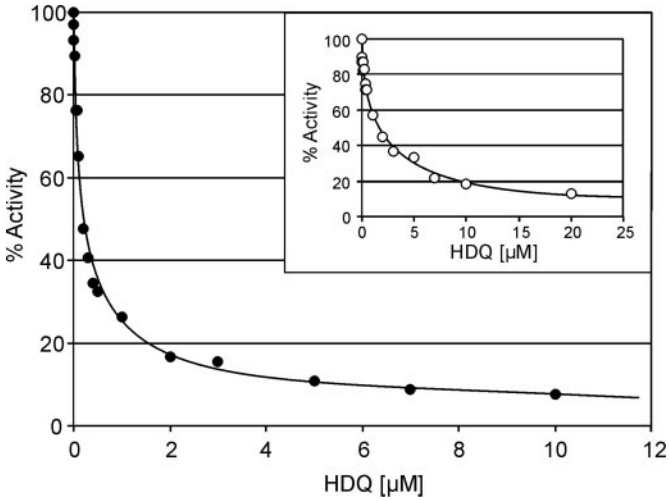

FIG. 2. **HDQ is a potent inhibitor of YLNDH2.** The concentration of 1-hydroxy-2-dodecyl-4(1*H*)quinolone required for half-maximal inhibition (I_{50}) of YLNDH2 was determined at a concentration of 30 μg/ml protein in the presence of 60 μM DBQ and 100 μM NADH. To selectively assay YLNDH2 activity, membranes of strain *nuam*Δ/pUB7 were used (IC_{50} = 200 nM). *Insert*, to selectively assay complex I activity, membranes of strain GB 5.2 were used (IC_{50} = 2 μM).

MATERIALS AND METHODS

Strains and Growth of Cells—Y. lipolytica strain PIPO (*NUGM*-Ht2, *lys*11–23, *ura*3–302, *leu*2–270, *xpr*2–322, *Mat*A (18)) was used for studies on the reaction mechanism. Complex I deletion strain *nuam*Δ/pUB 7 (*nuam*::*URA*3, *his*-1, *leu*2–270, *xpr*2–322, *NDH2i* (14)) and *NDH*2 deletion strain GB 5.2 (*ndh*2::*URA*3, *his*-1, *leu*2–270, *xpr*2–322, *Mat*B) were used for characterization of the inhibitor HDQ. *Y. lipolytica* cells were grown in complete medium (1% yeast extract, 2% peptone) with 2% glucose at 27 °C.

Preparation of Mitochondrial Membranes and Kinetic Measurements— 5–10 g of cells were vortexed 13 × 1 min in 10 ml of ice-cold 600 mM sucrose, 20 mM Na^+/Mops, pH 7.2, 1 mM EDTA, and 2 mM PMSF and 10 g of glass beads. After washing the glass beads with the same buffer, unbroken cells and cell fragments were sedimented at 2000 × *g* for 30 min. The supernatant was centrifuged again at 25,000 × *g* for 1 h to pellet mitochondrial membranes that were homogenized in a Potter-Elvehjem homogenizer, shock-frozen, and stored at −80 °C.

The steady-state NADH:DBQ oxidoreductase activity of membranes was measured as NADH oxidation at 340–400 nm (ϵ = 6.22 mM^{-1} cm^{-1}) or 366–400 nm (ϵ = 3.3 mM^{-1} cm^{-1}). The concentration of HDQ was measured at 329 nm (ϵ_{329} = 9.4 mM^{-1} cm^{-1}). To discriminate between NADH dehydrogenase activities in *Y. lipolytica* mitochondrial membranes, alternative dehydrogenase was measured in the presence of the complex I inhibitor DQA (2 μM) or using the complex I deletion strain *nuam*Δ/pUB 7. Complex I activity was determined using dNADH as electron donor, which is oxidized specifically by complex I (19) or NADH with the NDH2 deletion strain GB 5.2. Tests were carried out at 30 °C in 20 mM Na^+/Mops, 50 mM NaCl, and 2 mM KCN either in a stirred cuvette using a Photodiode array spectrophotometer (Multi Spec 1501, Shimadzu) or in a microtiter plate using a Microplate spectrophotometer (SPEKTRAmax® PLUS^{384}, Molecular Devices). The application of the Michaelis-Menten equation to enzymatic reactions involving highly hydrophobic substrates like ubiquinone in the presence of a membrane phase requires careful analysis of the primary data. In the case of alternative NADH dehydrogenase, we observed a non-linear dependence of the catalytic rate at low substrate concentrations. The data could not be fitted to either the standard Michaelis-Menten or to the Hill equation. Apparently, low concentrations of substrate were not available for reaction with alternative NADH dehydrogenase. The exact reason for this anomaly remained unclear. To deal with this experimental problem, we assumed that the substrate concentration [S] relevant for the rate *v* of alternative NADH dehydrogenase had to be corrected by an offset (in the range from 0 to 5 μM) that had to be determined for every data set. We corrected the added substrate concentration $[S]^{added}$ by this offset value *c* to obtain [S] as the substrate concentration available for binding and catalysis as shown in Equation 1.

$$[S] = [S]^{added} - c \qquad \text{(Eq. 1)}$$

When we applied this correction, the experimental data were described very well by standard steady state kinetic equations. Michaelis-Menten parameters and the offset value *c* were determined by direct fit using the ENZFITTER software package (Biosoft).

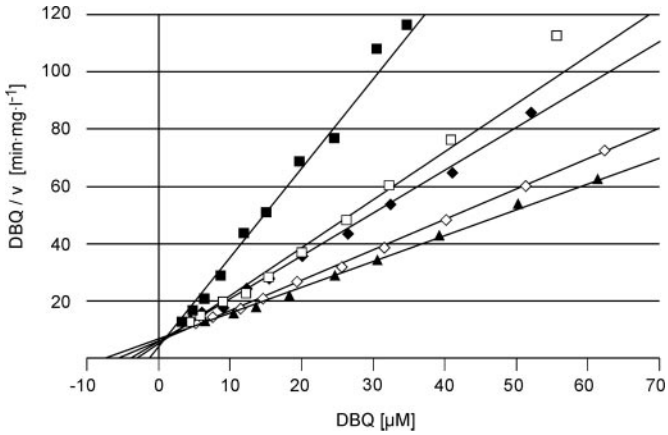

FIG. 3. **YLNDH2 employs a ping pong reaction mechanism.** Hanes plots ([S]/*v* over [S]) of steady-state kinetics with mitochondrial membranes of wild type strain PIPO (20 μg/ml total protein in each assay) are shown. V_{max} and apparent K_m values for DBQ in the presence of five different concentrations of NADH were obtained from direct fits to the Michaelis-Menten equation and used to calculate the lines. NADH concentrations were 10 (■), 20 (□), 30 (♦), 50 (◇), and 100 μM (▲). V_{max} values were 0.32 ± 0.02 (■), 0.60 ± 0.03 (□), 0.67 ± 0.02 (♦), 0.94 ± 0.02 (◇), and 1.11 ± 0.02 unit/mg (▲). Apparent K_m values for DBQ were 1.3 ± 0.4 (■), 3.0 ± 0.7 (□), 3.9 ± 0.6 (♦), 5.5 ± 0.6 (◇), and 7.4 ± 0.7 μM (▲). Each data point represents the mean ± S.D. of three independent measurements.

RESULTS

Reactivity of NDH2 with Different Electron Acceptors—We measured electron transfer rates with different electron acceptors to test the substrate specificity of alternative NADH dehydrogenase from *Y. lipolytica*. The activities were measured in the presence of 150 μM NADH and 60 μM of the respective

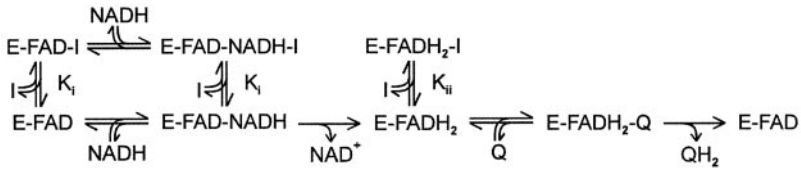

SCHEME 1

electron acceptor in four different preparations at a membrane concentration of 20 μg/ml (Table I). A rather high variability of the absolute specific activities seemed to reflect some variability in the quality of the mitochondrial membranes and possibly also variable expression levels of YLNDH2. However, relative to DBQ, the activities with the different electron acceptors were very similar in all of the preparations. Remarkably, the highest rates were obtained with hydrophilic ubiquinone-1 and not with DBQ, which with respect to its hydrophobicity came closest to the physiological substrate ubiquinone-9. Somewhat lower electron transfer rates were observed with duroquinone and bicyclic menadione. The artificial electron acceptor dichlorophenol-indophenol, which is known to accept electrons from many NADH-dependent dehydrogenases, also gave catalytic activities that were even higher than with DBQ.

HDQ Is a Potent Inhibitor of YLNDH2—In a search for potent inhibitors of alternative NADH dehydrogenase, we tested the inhibitory effect of HDQ (Fig. 1) on the NADH: ubiquinone oxidoreductase activity of *Y. lipolytica* mitochondrial membranes from strain *nuam*Δ/pUB 7 that lacks complex I. With DBQ as a substrate, 80–90% YLNDH2 activity was inhibited by 10 μM HDQ. Ubiquinone-1 reductase was inhibited to the same extent, but the inhibitor had no or only minor effects on the reduction rates of the other electron acceptors tested (Table I). Using the same assay with increasing inhibitor concentrations, we determined the HDQ concentration required for half-maximal inhibition of alternative NADH: ubiquinone oxidoreductase activity (IC_{50}) as 200 nM (Fig. 2). HDQ was found to also inhibit complex I decylubiquinone reductase activity in membranes from strain GB 5.2 lacking YLNDH2. However, at an IC_{50} of 2 μM, it acted ten times less efficiently on this enzyme (Fig. 2, *inset*).

YLNDH2 Bisubstrate Kinetics Suggest a Ping-Pong Reaction Mechanism—To determine the kinetic mechanism for NADH: DBQ oxidoreductase activity, we measured a series of bisubstrate kinetics of alternative NADH dehydrogenase. Mitochondrial membranes from strain PIPO in the presence of 2 μM DQA were assayed at increasing DBQ concentrations using five different concentrations of NADH. In a Hanes (20) diagram ([S]/v over [S] in Fig. 3), the lines crossed very close to the y axis. This is consistent with a ping-pong reaction mechanism for which ideally the lines cross on the ordinate. Enzymes that operate by a ping-pong mechanism cannot form a ternary complex with both substrates. A (random or ordered) sequential mechanism could be excluded, as in these cases the lines would cross in the fourth quadrant of the Hanes diagram. Based on this result of the bisubstrate kinetics, we applied Equation 2 for a ping-pong mechanism for further kinetic analysis.

$$v = \frac{V_{max}[\mathrm{NADH}][\mathrm{Q}]}{K_m^{\mathrm{Q}}[\mathrm{NADH}] + K_m^{\mathrm{NADH}}[\mathrm{Q}] + [\mathrm{NADH}][\mathrm{Q}]} \quad \text{(Eq. 2)}$$

Refined fitting of the experimental data (not shown) using this equation resulted in K_m values of 16.5 μM for NADH and 7.0 μM for DBQ.

HDQ Exhibits Non-competitive Inhibition Kinetics for Both Substrates of YLNDH2—To determine the inhibition mode of the quinolone derivative HDQ, we performed steady-state inhibition kinetics for both substrates of alternative NADH dehydrogenase, NADH and DBQ. Initial analysis of the data (not shown) clearly suggested non-competitive inhibition for both substrates with similar values for the two inhibition constants. This conclusion appeared counterintuitive, because one would have expected that the hydrophobic inhibitor HDQ would compete with the hydrophobic substrate DBQ for a similar domain on the enzyme. However, there is a case of bisubstrate kinetics for which the observed pattern is predicted, namely if an enzyme operates by a ping-pong mechanism and if the inhibitor blocks both the enzyme, in our case, oxidized YLNDH2 = *E*-FAD in Scheme 1, and the intermediate state, in our case reduced YLNDH2 = *E*-$FADH_2$ in Scheme 1 (21). Kinetic calculations, as described in the following, demonstrated that our data are consistent with a model in which the inhibitor also interacts with a complex consisting of enzyme and one of its substrates, presumably NADH. This situation is described by Scheme 1, where *E* is the enzyme, *I* is the inhibitor, Q is the oxidized, and QH_2 is the reduced quinone. The rate equation describing this situation (21) is shown in Equation 3.

$$v = \frac{V_{max}[\mathrm{NADH}][\mathrm{Q}]}{K_m^{\mathrm{Q}}[\mathrm{NADH}]\left(1 + \frac{[\mathrm{I}]}{K_{ii}}\right) + K_m^{\mathrm{NADH}}[\mathrm{Q}]\left(1 + \frac{[I]}{K_i}\right) + [\mathrm{NADH}][\mathrm{Q}]\left(1 + \frac{[I]}{K_i}\right)} \quad \text{(Eq. 3)}$$

When Equation 3 is inverted the following double-reciprocal form is obtained as shown in Equation 4.

$$\frac{1}{v} = \frac{1}{V_{max}} \times \frac{K_m^{\mathrm{Q}}}{[\mathrm{Q}]}\left(1 + \frac{[I]}{K_{ii}}\right) + \frac{1}{V_{max}} \times \frac{K_m^{\mathrm{NADH}}}{[\mathrm{NADH}]}\left(1 + \frac{[I]}{K_i}\right) + \frac{1}{V_{max}}\left(1 + \frac{[I]}{K_i}\right) \quad \text{(Eq. 4)}$$

Fig. 4 shows the corresponding double-reciprocal plots for inhibition kinetics with both substrates. As evident from increasing slopes and the fact that the lines do not intercept on the ordinate, inhibition kinetics were non-competitive for both substrates. If [NADH] is kept constant, the slope m in the double-reciprocal plots is given by Equation 5,

$$m = \frac{K_m^{\mathrm{Q}}}{V_{max}} + \frac{K_m^{\mathrm{Q}}}{V_{max} \times K_{ii}} \times [I] \quad \text{(Eq. 5)}$$

and, as Equation 4 is symmetrical for [Q] and [NADH], if [Q] is kept constant by Equation 6.

$$m = \frac{K_m^{\mathrm{NADH}}}{V_{max}} + \frac{K_m^{\mathrm{NADH}}}{V_{max} \times K_i} \times [I] \quad \text{(Eq. 6)}$$

The inhibition constants K_i and K_{ii} then can be derived directly from the x axis intercepts of the linear secondary plots m over [*I*] (Fig. 5*A*). The resulting inhibition constants were K_{ii} = 340 nM (Equation 5) and K_i = 290 nM (Equation 6). Thus, within experimental error, both dissociation constants are the same.

Similarly, the inhibition constants can be derived from the y axis intercepts b of the double reciprocal plots (Fig. 4) as shown in Equations 7 and 8.

$$b = \frac{1}{V_{max}}\left(\frac{K_m^{\mathrm{NADH}}}{[\mathrm{NADH}]} + 1\right) + \frac{1}{V_{max} \times K_i}\left(\frac{K_m^{\mathrm{NADH}}}{[\mathrm{NADH}]} + 1\right) \times [I]$$

for [NADH] = constant (Eq. 7)

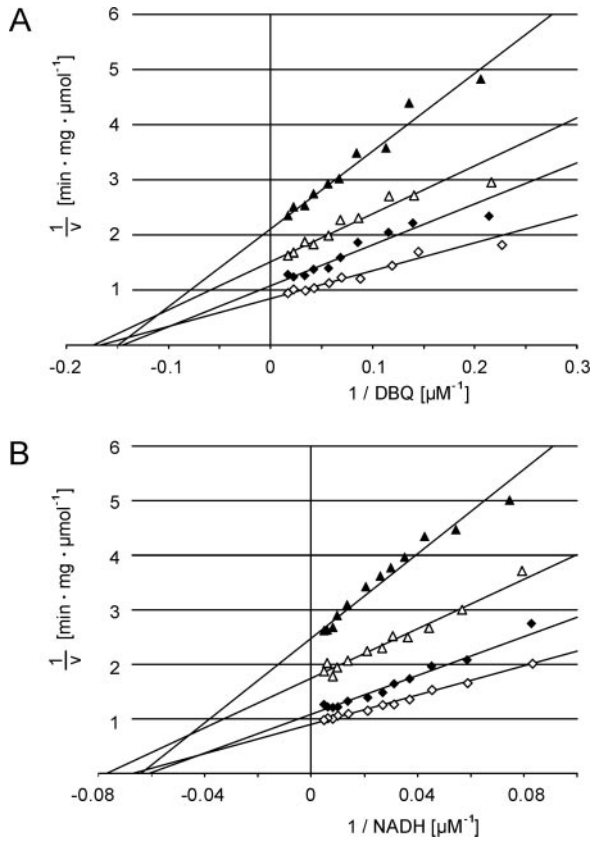

FIG. 4. **Double-reciprocal plots of HDQ inhibition kinetics of YLNDH2 in mitochondrial membranes.** Inhibition kinetics of strain PIPO (total protein concentration 20 μg/ml) for DBQ (*A*, 100 μM NADH) and NADH (*B*, 60 μM DBQ) were measured in the absence (◇) and in the presence of 50 (◆), 200 (△), and 500 nM HDQ (▲). The lines for the diagrams were calculated using parameters obtained from direct fits assuming a ping-pong mechanism. In *A*, V_{max} values were 1.18 ± 0.04 (◇), 0.92 ± 0.04 (◆), 0.66 ± 0.02 (△), and 0.47 ± 0.01 units/mg (▲). Apparent K_m values for DBQ were 5.99 ± 0.70 (◇), 6.89 ± 0.98 (◆), 5.76 ± 0.66 (△), and 6.66 ± 0.61 μM (▲). In *B*, V_{max} values were 1.11 ± 0.02 (◇), 0.92 ± 0.02 (◆), 0.57 ± 0.01 (△), and 0.40 ± 0.01 units/mg (▲). Apparent K_m values for NADH were 14.8 ± 1.1 (◇), 16.5 ± 1.5 (◆), 13.1 ± 1.1 (△), and 15.5 ± 1.6 μM (▲). Each data point represents the mean ± S.D. of three independent measurements.

$$b = \frac{1}{V_{max}}\left(\frac{K_m^Q}{[Q]} + 1\right) + \frac{1}{V_{max}}\left(\frac{K_m^Q}{[Q] \times K_{ii}} + \frac{1}{K_i}\right) \times [I]$$

for [Q] = constant (Eq. 8)

For Equation 7, the *x* axis intercept of the secondary plots *b* over [*I*] (Fig. 5*B*) directly gives the inhibition constant K_i as 380 nM. Equation 8 contains both inhibition constants and therefore only gives a unique solution if $K_i = K_{ii}$, but it can be derived from our previous kinetic analysis that this condition holds for HDQ and NDH2. The resulting inhibition constant then again can be derived directly from the *x* axis intercept as 300 nM. The mean dissociation constant for HDQ of 330 ± 40 nM derived from all four secondary plots fits rather well to the directly obtained IC_{50} value of ~200 nM (*cf.* Fig. 2).

A simulation (see supplementary material) based on the above kinetic model reveals that the IC_{50} value is critically affected by the steady-state concentration of *E*-$FADH_2$ that in turn depends on the ratio of the catalytic constants for the reduction of FAD and reoxidation of $FADH_2$, k_{cat}^{NADH} and k_{cat}^{Q}. Using the parameters obtained from the kinetic analysis, it can be deduced that quinone reduction should be at least ten times faster than NADH oxidation, which is likely to occur by hydride transfer.

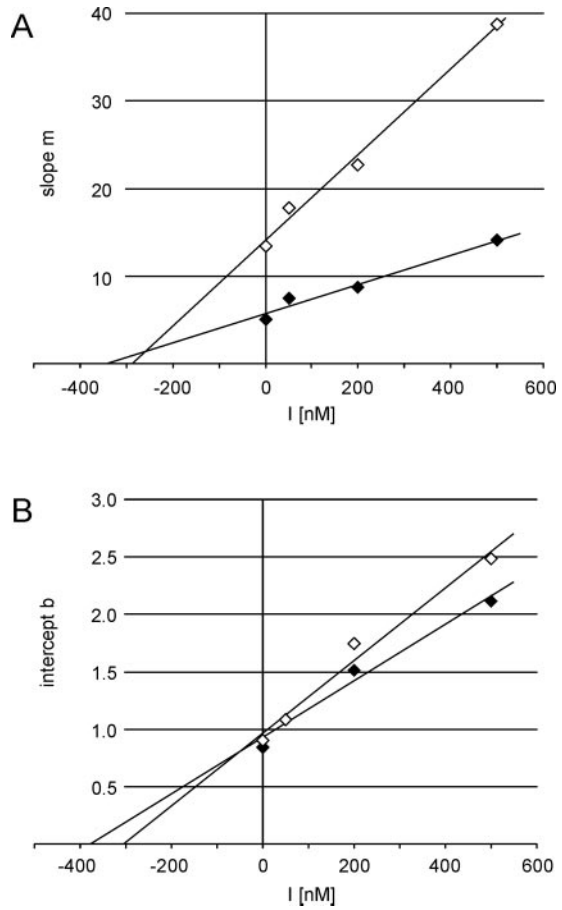

FIG. 5. **Secondary plots of HDQ inhibition kinetics of YLNDH2 in mitochondrial membranes.** Slopes (see Equations 5 and 7) (*A*) and *y* axis intercepts (see Equations 6 and 8) (*B*) from Fig. 4 were plotted against the inhibitor concentrations used in the DBQ (◆) and NADH (◇) inhibition kinetics. The inhibition constants K_i and K_{ii} were deduced from the *x* axis intercepts of the secondary plots (see "Results").

DISCUSSION

With an IC_{50} of 200 nM, HDQ is the most potent inhibitor of alternative NADH dehydrogenase identified so far. At 95 μM, the IC_{50} of the commonly used inhibitor flavone is almost 500-fold higher (4). As a hydrophobic quinolone derivative, HDQ was likely to act as ubiquinone analogue in a competitive manner. However, steady-state inhibition kinetics of HDQ followed a classical non-competitive pattern for both substrates, NADH and the hydrophobic ubiquinone derivative DBQ. This unexpected result could be explained based on a ping-pong mechanism that was deduced independently from the bisubstrate kinetics of alternative NADH dehydrogenase. Our data are consistent with a model in which the inhibitor HDQ shows competitive inhibition with the hydrophobic substrate DBQ and classical non-competitive inhibition with the hydrophilic substrate NADH. It should be noted that our data would also be consistent with a model in which both substrates are inhibited in a non-competitive fashion. However, this seems unlikely considering the structure and physicochemical properties of HDQ and ubiquinone. Moreover, the central conclusion that alternative dehydrogenase operates by a ping-pong mechanism would hold also in this case.

Results obtained by classical Michaelis-Menten kinetics have to be interpreted with great caution if membrane-associated enzymes are analyzed that react with highly hydrophobic substrates, as is the case for alternative NADH dehydrogenase. However, the fact that direct measurement of the IC_{50} value, inhibition kinetics, and bisubstrate kinetics gave fully consist-

ent results strongly supported our conclusion that the reaction of alternative NADH dehydrogenase with NADH and ubiquinone operates by a ping-pong mechanism. A ping-pong mechanism was also deduced from kinetic studies with partially purified SCNDI1 (22). However, these authors used the artificial hydrophilic electron acceptor dichlorphenol-indophenol as the second substrate. As indicated by the fact that this reaction is not inhibited by the quinone analogue HDQ (Table I), no conclusions on the physiological reaction mechanism can be drawn from this study.

The absence of a ternary complex of alternative NADH dehydrogenase, NADH, and ubiquinone implied by the ping-pong mechanism can be interpreted in two ways. 1) Either there are two independent binding sites that are linked by a very strong anti-cooperative effect, or 2) both substrates bind competitively to a common binding pocket of the enzyme. A strong anti-cooperative effect of the required type is rarely found, and it is hard to see why this would be required for the simple electron transfer reaction catalyzed by alternative NADH dehydrogenase. However, mutually exclusive binding of hydrophilic NADH and hydrophobic ubiquinone to a common binding pocket also does not seem very likely at first sight. Although a definitive answer cannot be given based on kinetic analysis, the observed substrate specificity clearly favors the latter option. The reactivity of alternative dehydrogenase with quinone-like compounds seems to have no specific requirements, as it was shown to catalyze the reduction of quite different electron acceptors with similar efficiency. The fact that HDQ could only inhibit the reaction if the electron acceptor carried a ubiquinone headgroup suggested that the different substrates interacted in rather different ways with the enzyme. Overall, this lends little support to an electron transfer mechanism involving strong anti-cooperativity that would imply highly specific binding interactions and strict control of the electron transfer reaction.

On the other hand, alternative NADH dehydrogenase seems not to discriminate too much between hydrophilic and hydrophobic quinones (Table I), suggesting that its actual active site interacts predominantly with the hydrophilic ubiquinone headgroup and that there may be no specific interaction with the hydrophobic tail of ubiquinone. This proposal is in line with the x-ray structure of the analogous mammalian quinone reductase QR1 (23) that catalyzes electron transfer from NAD(P)H to water soluble quinone-like compounds. Cocrystallization with NADPH and duroquinone revealed that both substrates bind in a similar fashion: The same side of the isoalloxazine ring of the FAD cofactor is stacked on to the duroquinone or the nicotineamide ring of NADPH. In summary, we conclude that alternative NADH dehydrogenase is highly likely to contain a common binding pocket for NADH and the ubiquinone headgroup.

REFERENCES

1. Kerscher, S. (2000) *Biochim. Biophys. Acta* **1459,** 274–283
2. Oettmeier, W., Masson, K., Soll, M., and Reil, E. (1994) *Biochem. Soc. Trans.* **22,** 213–216
3. Rasmusson, A. G., Svensson, A. S., Knoop, V., Grohmann, L., and Brennicke, A. (1999) *Plant J.* **20,** 79–87
4. de Vries, S., and Grivell, L. A. (1988) *Eur. J. Biochem.* **176,** 377–384
5. Kerscher, S., Okun, J. G., and Brandt, U. (1999) *J. Cell Sci.* **112,** 2347–2354
6. Melo, A. M., Duarte, M., and Videira, A. (1999) *Biochim. Biophys. Acta* **1412,** 282–287
7. Melo, A. M., Duarte, M., Möllers, I. M., Prokisch, H., Dolan, P. L., Pinto, L., Nelson, M. A., and Videira, A. (2001) *J. Biol. Chem.* **276,** 3947–3951
8. Björklöf, K., Zickermann, V., and Finel, M. (2000) *FEBS Lett.* **467,** 105–110
9. Matsushita, K., Otofuji, A., Iwahashi, M., Toyama, H., and Adachi, O. (2001) *FEMS Microbiol. Lett.* **204,** 271–276
10. Gomes, C. M., Bandeiras, T. M., and Teixeira, M. (2001) *J. Bioenerg. Biomembr.* **33,** 1–8
11. Bandeiras, T. M., Salgueiro, C., Kletzin, A., Gomes, C. M., and Teixeira, M. (2002) *FEBS Lett.* **531,** 273–277
12. Bandeiras, T. M., Salgueiro, C. A., Huber, H., Gomes, C. M., and Teixeira, M. (2003) *Biochim. Biophys. Acta* **1557,** 13–19
13. Luttik, M. A. H., Overkamp, K. M., Kötter, P., de Vries, S., van Dijken, P., and Pronk, J. T. (1998) *J. Biol. Chem.* **273,** 24529–24534
14. Kerscher, S., Eschemann, A., Okun, P. M., and Brandt, U. (2001) *J. Cell Sci.* **114,** 3915–3921
15. Lesk, A. M. (1995) *Curr. Biol.* **5,** 775–783
16. Mattevi, A., Schierbeek, A. J., and Hol, W. G. J. (1991) *J. Mol. Biol.* **220,** 975–994
17. Mattevi, A., Obmolova, G., Sokatch, J. R., Betzel, C., and Hol, W. G. J. (1992) *PROTEINS: Struct. Funct. Bioinf.* **13,** 336–351
18. Kerscher, S., Dröse, S., Zwicker, K., Zickermann, V., and Brandt, U. (2002) *Biochim. Biophys. Acta* **1555,** 83–91
19. Matsushita, K., Ohnishi, T., and Kaback, H. R. (1987) *Biochemistry* **26,** 7732–7737
20. Hanes, C. S. (1932) *Biochem. J.* **26,** 1406–1421
21. Cleland, W. W. (1963) *Biochim. Biophys. Acta* **67,** 173–187
22. Velásques, I., and Pardo, J. P. (2001) *Arch. Biochem. Biophys.* **389,** 7–14
23. Faig, M., Bianchet, M. A., Talalay, P., Chen, S., Winski, S., Ross, D., and Amzel, L. M. (2000) *Proc. Natl. Acad. Sci. U. S. A.* **97,** 3177–3182